

Cite this: DOI: 10.1039/c2lc21164e

www.rsc.org/loc

CRITICAL REVIEW

Microfluidic synthesis of advanced microparticles for encapsulation and controlled release†

Wynter J. Duncanson,^a Tina Lin,^a Adam R. Abate,^b Sebastian Seiffert,^{cd} Rhutesh K. Shah^e and David A. Weitz^{*a}

Received 25th November 2011, Accepted 7th March 2012

DOI: 10.1039/c2lc21164e

We describe droplet microfluidic strategies used to fabricate advanced microparticles that are useful structures for the encapsulation and release of actives; these strategies can be further developed to produce microparticles for advanced drug delivery applications. Microfluidics enables exquisite control in the fabrication of polymer vesicles and thermosensitive microgels from single and higher-order multiple emulsion templates. The strategies used to create the diversity of microparticle structures described in this review, coupled with the scalability of microfluidics, will enable fabrication of large quantities of novel microparticle structures that have potential uses in controlled drug release applications.

A Introduction

The goal of advanced drug delivery is to supply doses of drugs for sustained periods to specific sites in the body;^{1,2} this can be achieved by efficiently loading drugs into microparticles and controllably releasing them when the microparticles have reached their specified target location.^{1,3} To regulate the release of the drug, it is critical to controllably produce microparticles with known sizes and size distributions since the rate of drug release is proportional to microparticle size.^{4–8} Another way to achieve controlled release is to trigger the release of the drugs; this can be accomplished by using stimulus-responsive materials that undergo a physicochemical change in response to environmental triggers such as pH, temperature or ionic strength.^{9,10} Further tuning of drug release can also be attained by tailoring the internal structure of the microparticles. For example, adjusting the size and number of internal compartments allows simultaneous delivery of multiple drugs. Alternatively, increasing the thickness of the shell of a core-shell structure microparticle will increase the diffusion path and decrease the rate of release of

the drug. In addition, ideally, the drug should be encapsulated with 100% efficiency. However, conventional high-shear emulsification techniques used to fabricate microparticle drug carriers, such as precipitation, spray-drying, and phase separation,^{4–6,11,12} produce microparticles that have a large polydispersity in size, a high variability in structure, and a wide range of encapsulation efficiencies.

One potentially promising approach to overcome these limitations is through use of droplet microfluidics to produce highly-controlled and uniform emulsion-based templates which can then be used for the formation of microparticles for encapsulation and controlled release applications such as drug delivery. Using microfluidic devices, streams of immiscible fluids can be combined to create single, double, and higher-order emulsions with an exquisite degree of control. The chemical composition of the resultant drops can be varied through the use of a wide range of constituent fluids. The flexibility of material choice, combined with the diversity of emulsion-order, greatly broadens the range of microparticles that can be produced. The control and versatility afforded by microfluidics makes this technique ideal for fabrication of advanced microparticles that can be modified to produce highly-complex drug delivery vehicles. However, for these strategies to be truly useful, the low production rates typical of microfluidics must be increased and this requires significant ‘scale-up’ through parallelization of the microfluidic networks.

In this review, we highlight work from our lab in which we use droplet microfluidic strategies to prepare highly-controlled microparticle structures from emulsion templates. We describe glass capillary microfluidic devices and their use in the fabrication of several different structures as model systems for encapsulation and controlled release; these include polymerosomes, or polymer vesicles, and poly(*N*-isopropylacrylamide) (pNIPAm) microgel microparticles. We also present a variety of

^aSchool of Engineering and Applied Sciences/Department of Physics, Harvard University, Cambridge, Massachusetts, USA.

E-mail: weitz@seas.harvard.edu; wynterjd@seas.harvard.edu; tinalin@fas.harvard.edu; Tel: +1 617-495-3275

^bUCSF School of Pharmacy, Department of Bioengineering and Therapeutic Sciences, San Francisco, CA, USA.

E-mail: adam.abate@ucsf.edu; Tel: +1 415-476-9819

^cFreie Universität Berlin, Takustr. 3, D-14195 Berlin, Germany.

E-mail: seiffert@chemie.fu-berlin.de; Tel: +49 30 838 56082

^dHelmholtz Zentrum Berlin, F-12 Soft Matter and Functional Materials Hahn-Meitner-Platz 1, D-14109 Berlin, Germany.

E-mail: sebastian.seiffert@helmholtz-berlin.de; Tel: +49 30 8062 42294

^eShell Oil Company/Innovation Research and Development (IRD),

Westhollow Technology Center, Houston, TX 77082

E-mail: rhutesh.shah@shell.com; Tel: +1 281-544-7140

† Published as part of a LOC themed issue dedicated to research from the USA: Guest Editors Don Ingber and George Whitesides.

microparticle structures which we create by manipulating fluid flow rates and device geometries. Furthermore, we describe the production of these microparticles in PDMS microfluidics to show the potential for 'scale-up'.

B Microfluidic devices

We use microfluidic devices to produce emulsions, which are used as templates to create advanced microparticles for encapsulation and controlled release applications. The control afforded by microfluidics enables production of highly-controlled emulsions that serve as the precursors of these microparticles. Glass capillaries are one class of device that enables production of monodisperse emulsions. These devices consist of coaxial assemblies of a series of glass capillaries which have inherent advantages in that their wettability can be easily and precisely controlled and that they are rigid and chemically resistant; their truly three-dimensional geometry enables controlled fabrication of multiple emulsions. Single emulsion devices are constructed from a tapered round glass capillary that is inserted into a square glass capillary. In the co-flow geometry, the two fluid phases flow in the same direction; the dispersed phase flows inside the round capillary and the continuous phase flows between the square and round capillaries,^{13,14} as illustrated in Fig. 1a. Individual drops are produced periodically at the orifice of the round glass capillary. Alternatively, in the flow-focusing geometry,^{15,16} the dispersed phase is flowed inside the square capillary and the continuous phase is flowed between the square and round capillary in the opposite direction, as shown in Fig. 1b. The dispersed phase is focused by the continuous phase through the narrow orifice of the tapered round capillary; this process of flow-focusing generates emulsions in the collection capillary. Single emulsions can be produced using either the co-flow or flow-focusing geometry, while double emulsions are generally produced using a combination of the two geometries. A common device used to produce double emulsions consists of two round capillaries arranged end-to-end within a square

capillary¹⁶ as shown in Fig. 1c. The inner fluid is pumped through the tapered-round capillary while the middle fluid, co-flows through the outer square capillary. The outermost fluid flows through the outer square capillary in the opposite direction to flow-focus the coaxially flowing stream of the other two fluids. A double emulsion is formed when the three fluids enter the collection tube.

A drawback of glass capillary devices is that the manual fabrication makes it difficult to reproducibly construct more than one device at a time; thus the production of many identical devices is nearly impossible. To overcome this limitation, microfluidic devices made using soft-lithography in the silicon elastomer, poly(dimethylsiloxane) (PDMS), are used. PDMS device production is inherently parallel and precise, therefore, these devices can easily be replicated in large quantities; this makes them attractive for large-scale synthesis. An additional advantage of the PDMS device fabrication process is the flexibility to tailor the channel networks to make even more sophisticated drops-in-drops; these can be transformed into highly functional advanced drug delivery microparticles.

For these strategies to be commercially achievable, large quantities of these microparticles must be produced; however, a challenge in commercializing these strategies and techniques is the low production yields: current systems typically produce only microlitres-to-millilitres of product per hour. One approach to increase yield is to parallelize the devices. Rather than only a single dropmaker operating at a time, thousands or hundreds-of-thousands could be used in parallel; however, this would require separate sets of pumps to supply fluids to each device. Alternatively, multiple copies of dropmakers can be integrated into a single PDMS microfluidic device design that is integrated with fluid distribution channels;¹⁷ thus, a single set of syringe pumps is used to supply fluids to the device. This is achieved by repeating the dropmaker in both a two-dimensional and a three-dimensional array, and connecting them to a three-dimensional network of much larger distribution and collection channels. By operating 15 parallel devices simultaneously with production rates of 1 mL h^{-1} , droplets can be produced at increased rates of over 1 kg day^{-1} ; this should increase production rates to the levels needed for scaled production.

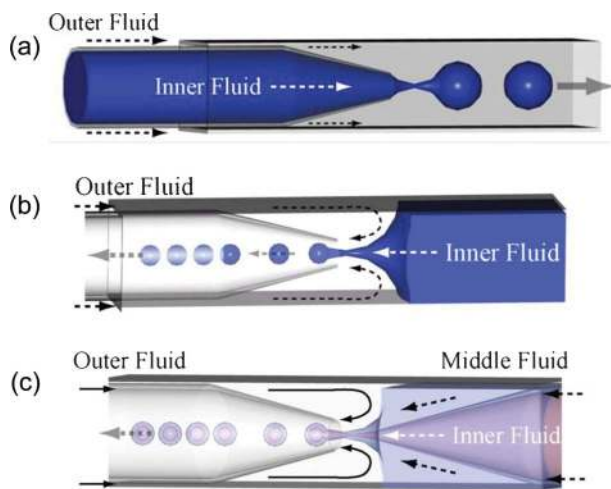


Fig. 1 (a) Schematic of a co-flow glass capillary device for making single emulsion droplets. Arrows indicate the flow direction of fluids and drops. (b) Schematic of a flow-focusing capillary device for making single emulsion droplets. (c) Schematic of a double emulsion capillary microfluidic device that combines co-flow and flow focusing.

C Polymersomes

An example of a common microparticle is a vesicle;¹⁸ this is a compartment of one fluid enclosed by a bilayer of amphiphilic molecules such as phospholipids, diblock copolymers, or polypeptides. The bilayer induces semi-permeability of the membrane; the hydrophobic components block passage of large molecules, whereas, the hydrophilic components allow transit of small molecules, such as water. Vesicles can be inflated or deflated in response to an osmotic pressure difference between the aqueous and surrounding environment. Moreover, the rates of inflation and deflation can be tuned by varying the thickness of the bilayer membranes. As membrane thickness increases, water permeability decreases and mechanical stability increases. For controlled release applications, vesicles with tunable permeability and excellent mechanical stability are required; therefore, polymer vesicles, or polymersomes are highly attractive.

Polymersomes are traditionally prepared by techniques that rely on the spontaneous self-assembly of amphiphiles. These techniques produce polymersomes that have high polydispersity and low encapsulation efficiency thus limiting their utility. To overcome these limitations, microfluidic devices can be used to produce polymersomes from water-in-oil-in-water (W/O/W) double emulsion templates; by independently controlling the flow rates of the fluids used, highly monodisperse double emulsions with high encapsulation efficiency are formed.^{19–22}

We use the double emulsion glass capillary device to produce monodisperse W/O/W double emulsions using an aqueous solution as the inner water phase, poly(ethylene-glycol)-*b*-polylactic acid (PEG-*b*-PLA) in a solvent mixture as the oil phase, and a surfactant solution as the outer water phase. After generation of double emulsions, the PEG-*b*-PLA adsorbs at the oil–water interfaces and the oil phase dewets to form monodisperse polymersomes upon solvent evaporation,²⁰ as shown in the series of images in Fig. 2a. After the dewetting process, the polymersomes still have a low polydispersity of only 4% or lower, as shown in the histogram in Fig. 2b. By controlling the relative flow rates of the fluids during drop formation, we can adjust the outer diameter of the polymersomes; this highlights the control that is achieved from microfluidic fabrication of polymersomes.

We demonstrate the potential for encapsulation and release of a model active, 4000 Da MW FITC–dextran, from these polymersomes. The molecules remain in the internal compartments as shown in Fig. 2c and is then released in response to a difference in osmotic pressure. A large and sudden osmotic pressure difference causes the polymersomes to quickly rupture; this occurs on a timescale that is too rapid to visualize. However, release can be visualized by minimizing the osmotic gradient; this is achieved by slowly evaporating the water in the outer water-phase of the

double emulsion. The increase in the concentration of the outer phase drives water out of the polymersome which causes it to shrink and buckle,²⁰ as shown in the series of images in Fig. 2d. Integration of different block ratios of diblock copolymers in the controlled fabrication process enables precise tuning of polymersome membrane thickness and permeability.

Advances in microfluidics enable generation of polymersomes that contain multiple compartments.²¹ These multi-compartment polymersomes have great potential for storing multiple drugs in a single carrier to enable simultaneous release of two actives. We produce these polymersomes using the same W/O/W double emulsion glass capillary devices shown in Fig. 1c used to generate single-component polymersomes. We precisely encapsulate multiple inner aqueous drops into one outer drop. After solvent evaporation, the copolymers at the inner water–oil (W/O) and the outer water–oil (O/W) interface form membranes with each other; this causes droplet adherence which leads to the formation of multi-compartment polymersomes, as illustrated in Fig. 3.

To demonstrate the encapsulation of two distinct active components in these multi-component polymersomes,²¹ we use a modified glass capillary devices shown in Fig. 4a to prepare polymersomes that contain two actives. The round injection capillary contains two separate channels that isolate the two active materials prior to their co-encapsulation. Two inner aqueous phase solutions of FITC–dextran and PEG are flowed in the two channels of the inner capillary and subsequently encapsulated in the outer phase; thus, double emulsions that contain two distinct aqueous drops are formed. After solvent evaporation, polymersome formation occurs and the two dyes are encapsulated in their individual compartments as seen in Fig. 4b; this confirms the encapsulation of two distinct encapsulants.

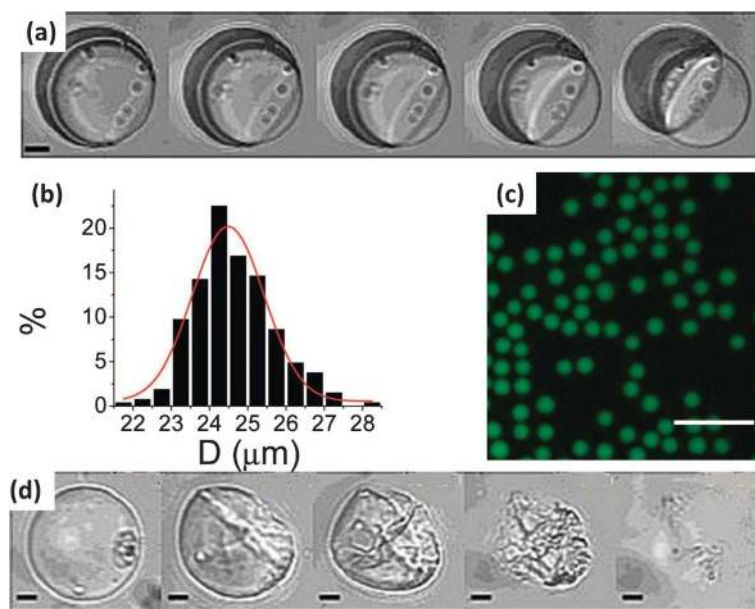


Fig. 2 (a) Dewetting transition of a double emulsion drop. Successive images are taken at intervals of 910 ms. (b) Size distribution of the PEG(5000)-*b*-PLA(5000) polymersomes. Polydispersity of polymersomes is 4.0%. The experimental data is fitted with a Gaussian distribution in red. (c) Encapsulation of a fluorescent dye in polymersomes. Scale bar is 100 μm . (d) Shrinkage and breakage of a polymersome after an osmotic shock. The scale bar is 10 μm . Reprinted with permission from ref. 20. Copyright 2008, American Chemical Society.

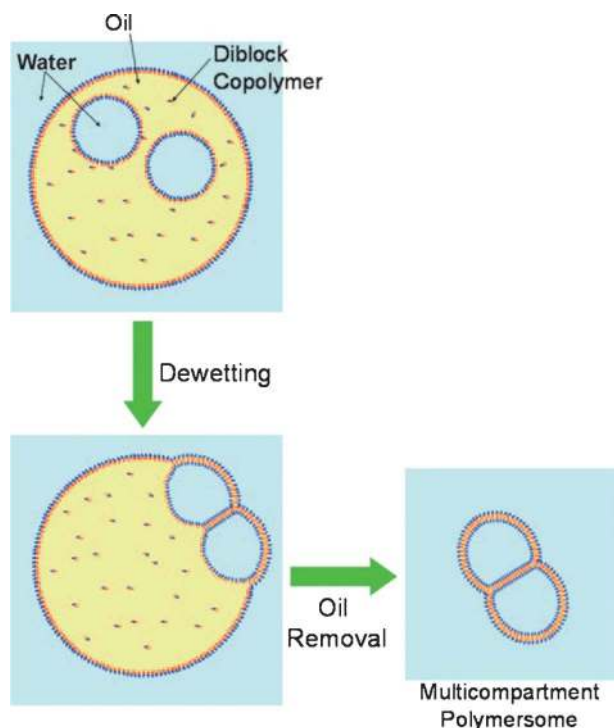


Fig. 3 Schematic of the generation of double emulsion drops with multiple inner droplets in a glass capillary microfluidic device. Reproduced from ref. 21. Copyright, 2011 WILEY-VCH Verlag GmbH & Co. KGaA, Weinheim.

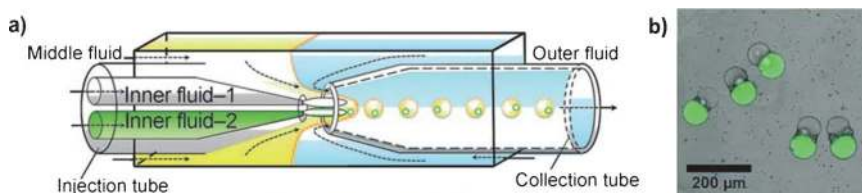


Fig. 4 (a) Capillary microfluidic device for preparing double emulsions with two distinct inner phases. (b) Overlay of optical microscope images and fluorescence microscope images of a monodisperse population of PEG(5000)-*b*-PLA(5000) polymersomes encapsulating FITC-dextran and PEG separately in their two compartments. Reproduced from ref. 21. Copyright, 2011 WILEY-VCH Verlag GmbH & Co. KGaA, Weinheim.

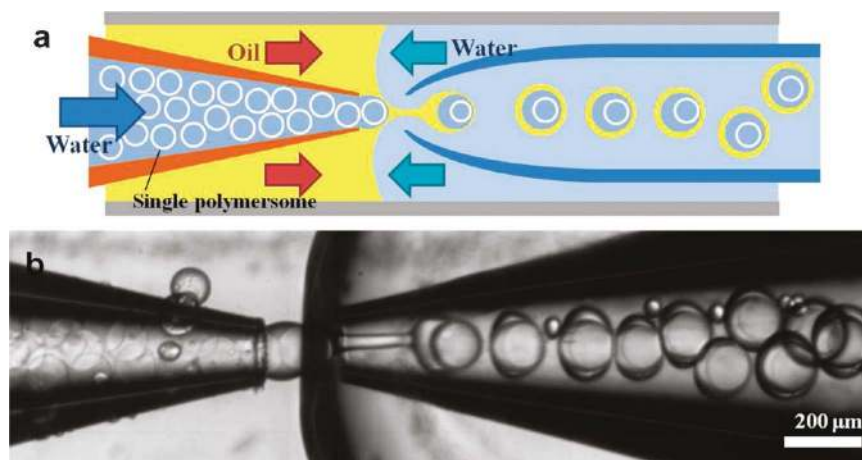


Fig. 5 (a) Schematic illustration of the microfluidic device for preparation of double polymersomes containing a single inner polymersome. (b) Optical microscope image showing injection of polymersomes into the innermost drops of double-emulsion drops, where the breakup of the middle phase is triggered by the polymersomes. Reprinted with permission from ref. 19. Copyright 2011, American Chemical Society.

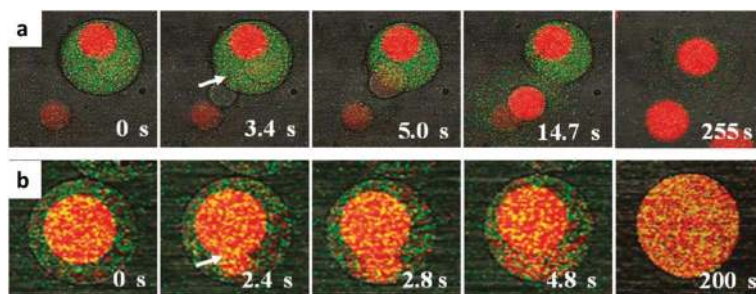


Fig. 6 (a) Series of confocal images showing selective dissociation of the outer membrane of double polymersomes, consisting of a poly(lactic acid) (PLA)-homopolymer-free bilayer for both the inner and outer membranes, in a mixture of water and ethanol at a volume ratio of 1 : 1. (b) Series of confocal images showing selective dissociation of the inner membrane of double polymersomes, consisting of a PLA-homopolymer-free bilayer for the inner membrane and a PLA-homopolymer-loaded bilayer for the outer membrane, in the same mixture of water and ethanol. Reprinted with permission from ref. 19. Copyright 2011, American Chemical Society.

homo-polymer, PLA, with the diblock in the outermost polymersome layer. The ethanol–water mixture in the surrounding environment disrupts the inner polymersome bilayer first to cause release of its contents into the outer polymersome. Then, as the PLA in the outermost polymersome degrades by hydrolysis, both actives from the inner and outer polymersome are released simultaneously as shown in the series of images in

Fig. 6b. Tuning of the polymersome composition enables simultaneous or sequential release. The encapsulation and programmed release described here is not limited to two actives, but is easily extended to multiple actives; this is achieved by producing higher order polymersomes-in-polymersomes and tuning membrane stability by changing its composition. The control afforded by microfluidics to change the number of

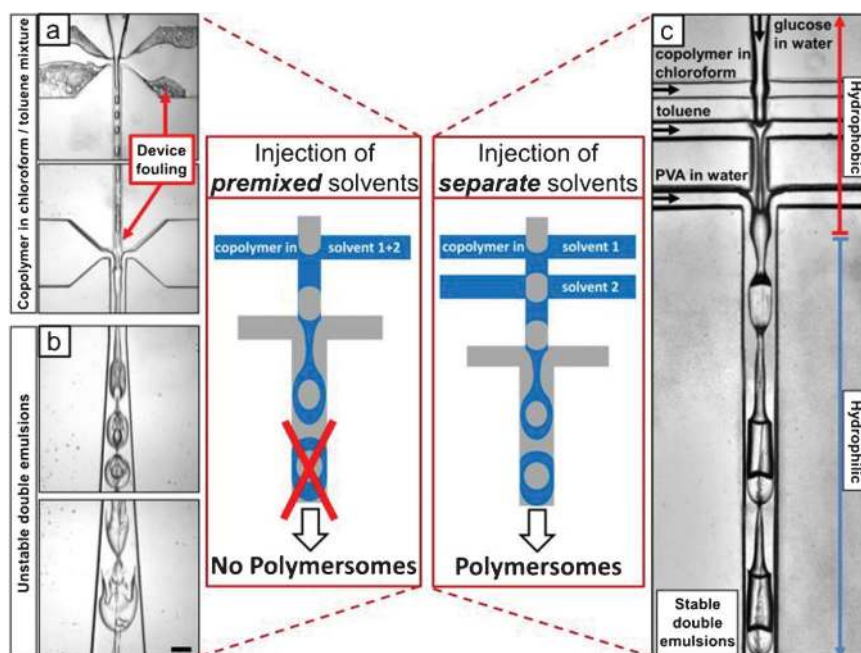


Fig. 7 Formation of copolymer-stabilized W/O/W double emulsions using a conventional microfluidic device with two cross junctions for injecting premixed organic solvents (left), and using a novel device design allowing separate injection of organic solvents (right). The microfluidic devices are sol-gel-coated to increase the resistance of the channel walls against organic solvents. The sol-gel coating in the upper half of the device is hydrophobic, while the coating in the lower part is rendered hydrophilic due to functionalization by grafted poly(acrylic acid). (a, b) Formation of PEG-*b*-PLA stabilized W/O/W double emulsions using premixed mixtures of toluene and chloroform. (a) Most of the diblock copolymer forms a precipitate after the more volatile chloroform starts to evaporate in the microfluidic device. The precipitates adhere to the surface of the channels, building up a thick layer. (b) Some of the precipitates are observed in the shell phase of the double-emulsion drops formed. Since the organic solvent phase is depleted of the copolymer before the formation of double emulsions occurs, the two interfaces of the shell inside the double emulsions are not sufficiently stabilized. Thus the double-emulsion droplets burst downstream. (c) Novel microfluidic device forming PEG-*b*-PLA stabilized W/O/W double emulsions. To maintain the stability of the polymersomes, the osmolarity of the inner and outer phase of the double emulsion templates is balanced by adding glucose to the inner phase and polyvinyl alcohol (PVA) to the outer phase. The non-Newtonian nature of the PVA solution causes the middle phase to develop a tail, which initially connects the double emulsions. However, the jet breaks up into stable double emulsion droplets approximately 1 mm downstream in the outlet channel. Scale bar for all panels denotes 100 μm . Adapted with permission from ref. 22. Copyright 2010 Wiley-VCH Verlag GmbH & Co. KGaA.

polymersomes-in-polymersomes, coupled with the tunability of polymersome stability achieved by varying material composition, opens new opportunities for advanced drug delivery polymersomes.

To produce polymersomes in large quantities, PDMS devices are required.²² Injection of the diblock in the solvent mixture into the channels of the PDMS device leads to precipitation of the diblock on the channel walls; this fouling changes the wettability of the channels and ultimately prevents the formation of double emulsions, as shown in a failing device in Fig. 7a and 7b. To overcome this challenge, we design and use a PDMS device²² with two separate inlets: one for the good solvent and the diblock, and the other for the bad solvent. By separating the solvents, diblock precipitation is prevented because the two streams only mix after they are encapsulated by the outer continuous phase as shown in Fig. 7c. We can tune the ratio of the two solvents in the device by independently controlling the fluid flow rates with syringe pumps. This allows us to obtain solvent ratios that normally could not be used in polymersome synthesis because of precipitation; this capability is important for forming vesicles from other copolymers.

We have shown that we can use glass capillary microfluidic devices to produce highly-controlled polymersomes. By changing flow rates, altering the devices, or reinjecting polymersomes into unmodified devices, we can produce sophisticated structures that can encapsulate and release multiple actives. We have also shown that we can produce single-compartment polymersomes in PDMS devices. By producing these highly controlled polymersomes in PDMS, we have great potential to scale-up production of these fascinating advanced polymersomes for encapsulation and controlled release.

D PNIPAm microgels

Hydrogels can hold large amounts of water or other water-soluble molecules because they are hydrophilic. They can be formed into spherical microparticles that entrap actives in their cross-linked networks.^{23,24} Microgels composed of stimulus-responsive materials can release actives in response to environmental triggers. One example is the use of pNIPAm to create thermosensitive microgels. PNIPAm synthesis entails a redox reaction of the *N*-isopropylacrylamide (NIPAm) monomer that is initiated by heat, UV or the addition of a catalyst. PNIPAm exhibits lower critical solution temperature behaviour: In water below 32 °C, hydrogen bonds form between the hydrophilic amine chains; this forces water into the polymer leading to swelling of the structure. By contrast, at higher temperatures, the hydrogen bonds are disrupted, which causes the pNIPAm to shrink. This makes pNIPAm an ideal model system for environmentally-triggered release: water-soluble actives can be encapsulated in pNIPAm microparticles and then be released from these structures in response to temperature changes. We can use the control afforded by microfluidics to synthesize monodisperse pNIPAm microgels with various internal structures. By changing the internal structures, we can alter the volume-phase kinetics to control release.

We use a glass capillary single-emulsion device that consists of two sets of co-flow geometries.²⁵ An aqueous pre-gel mixture of NIPAm, bis-acrylamide (BIS), and ammonium persulfate is

pumped through the cylindrical glass capillary and emulsified by a co-flowing oil phase of kerosene to form uniform droplets in the first co-flow geometry. The continuous phase that contains the initiator, *N,N,N',N'*-tetramethylethylenediamine (TEMED), is flowed between the outer coaxial region between the second square capillary and the right end of the tapered cylindrical capillary of the second co-flow geometry, as shown in Fig. 8a. The initiator diffuses into the aqueous droplet to trigger the redox reaction which causes simultaneous polymerization and subsequent polymerization of NIPAm.

The resultant microgels exhibit excellent thermal response, thereby enabling the release of actives in response to an increase in temperature,²³ when heated, their diameter is reduced to less

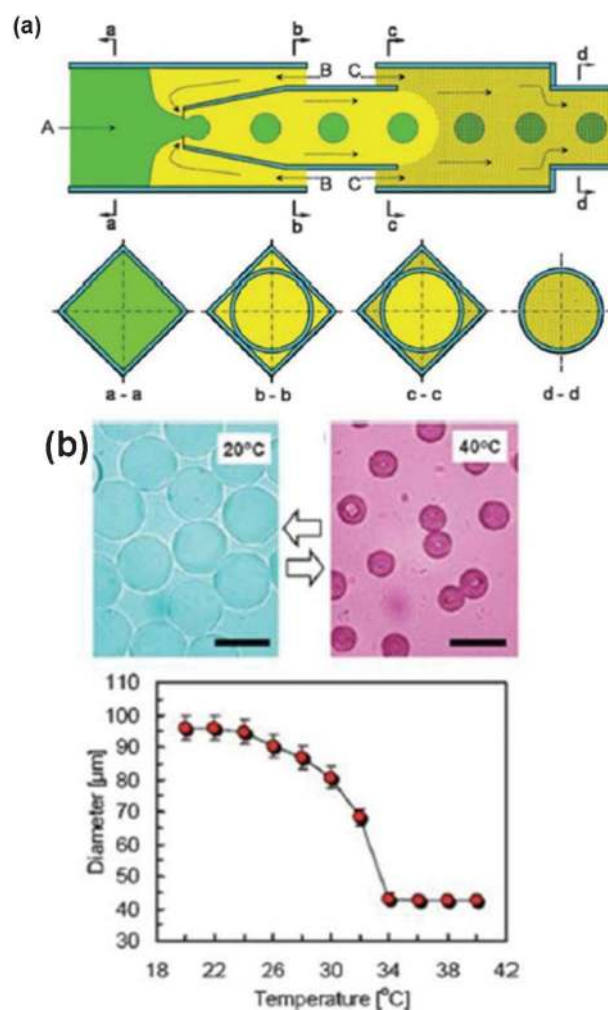


Fig. 8 (a) Schematic illustration of a capillary-based microfluidic device for fabricating monodisperse pNIPAm microgels. Fluid A is an aqueous suspension containing the monomer, crosslinker, and initiator; fluid B is an oil, and fluid C is the same oil as fluid B but contains a reaction accelerator that is both water- and oil-soluble. The accelerator diffuses into the drops and polymerizes the monomers to form monodisperse microgels. Cross-sectional views at different points along the device length are shown in the second row. (b) Size change of pNIPAm microgels in water triggered by changing the temperature. The scale bar is 100 μm. (a) Reprinted with permission from ref. 25. Copyright, 2007 WILEY-VCH. (b) Ref. 23—Reproduced by permission of The Royal Society of Chemistry.

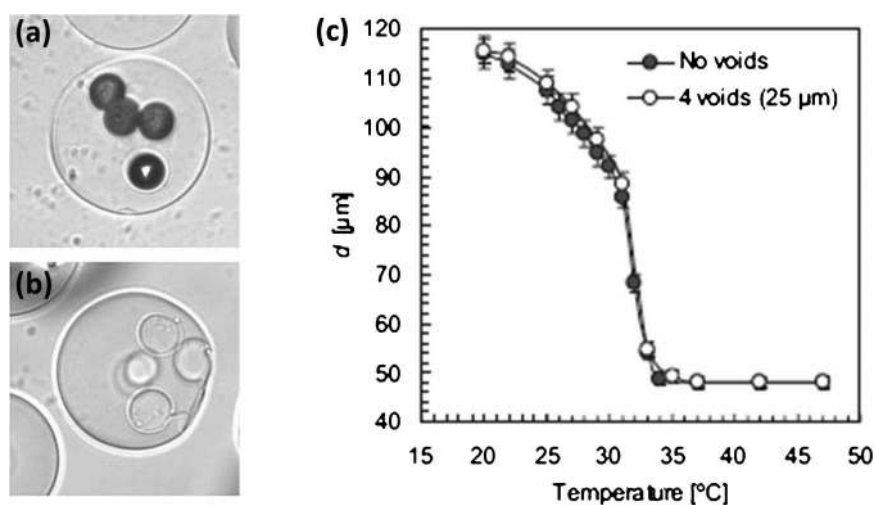


Fig. 9 (a) Microgels with embedded polystyrene beads. (b) Microgels with spherical voids formed by dissolving the embedded beads from such microgels. The scale bar is 100 μm . (c) Time-dependent diameter of microgels with different internal structures upon heating from 23 to 47 $^{\circ}\text{C}$. Reprinted with permission from ref. 25. Copyright, 2007 WILEY-VCH.

than half the original diameter, as shown in Fig. 8b. This size change is reversible and reproducible over several cycles. In addition, we can also incorporate voids inside the microgels by embedding polymeric particles inside the microgel solution prior to emulsification,²⁵ as shown in Fig. 9a; subsequent particle dissolution produces voids, shown in Fig. 9b. Incorporation of voids improves the rate of size change of the microgels because their kinetics are a function of the rate of diffusion of water through the microgels, as shown in Fig. 9c. The control afforded by microfluidics enables production of pNIPAM microgels, and microgels with voids that are useful for heat-triggered release.

Similar microgels can also be generated through controlled crosslinking of pre-fabricated pNIPAM polymer chains. To demonstrate this concept, we use pNIPAM chains which are functionalized with dimethylmaleimide (DMMI) side groups, a moiety that can be selectively transformed into dimers by UV irradiation,^{26,27} thereby crosslinking the chains. We prepare these precursors by copolymerizing *N*-isopropylacrylamide and a DMMI-functionalized acrylamide-derivative in a free-radical reaction in water, and we control the molecular weight of the resultant copolymers by performing this polymerization in the presence of sodium formate.²⁸ Once formed, the resultant crosslinkable precursor polymers are used to create pre-microgel droplets in a microfluidic device. We emulsify aqueous precursor solutions with polymer concentrations in the semidilute unentangled regime, an intermediate range above the threshold for coil overlap, c^* , yet below the onset of chain entanglement, c_e^* ; these experimental conditions guarantee that a space-filling polymer network can be formed inside each droplet, while ensuring that the viscosity of the polymer solution is not too high. After forming pre-microgel droplets, microgel particles are obtained by droplet gelation that is achieved through photocrosslinking of the precursor polymers in the drops. The advantage of this approach of particle fabrication is that it separates the polymer synthesis from the particle gelation; this allows each to be controlled independently, thus enabling microgel particles to be formed with well-controlled composition and functionality.²⁸

We can use colloidal pNIPAM microgels as building blocks to fabricate monodisperse colloidosomes, microcapsules with a shell composed of tightly packed colloidal particles.²⁹ Prior to emulsification, a small amount of glutaraldehyde is added to the aqueous mixture of amine-functionalized sub-micrometre-sized pNIPAM microgels that is emulsified in oil using a single-emulsion flow-focusing microfluidic device. The colloidal pNIPAM microgels assemble at the oil–water interface within the emulsion droplets due to the presence of hydrophobic isopropyl groups and hydrophilic acrylamide groups. Glutaraldehyde molecules link the amine-functionalized microgels through an amine–aldehyde condensation reaction to interlock the microgels at the oil–water interface, thereby forming colloidosomes. The overall schematic is presented in Fig. 10a. Such colloidosomes exhibit thermosensitive behaviour similar to that displayed by their constituent microgels: when the temperature is increased above the phase-transition temperature of pNIPAM, the diameter of the colloidosomes decreases by 42%, which roughly translates to an 80% decrease in volume, as shown in Fig. 10b. Thus, colloidosomes fabricated by microfluidics can be of immense potential in applications that require targeted pulsed-release of actives.

The ability to encapsulate controlled numbers of microgels into drops provides a powerful means to template multi-layered microgel particles.³⁰ We can also produce higher-order multiple emulsions using devices that consist of co-flow junctions that are followed by one or more additional co-flow junctions as illustrated in Fig. 11a. Hierarchical levels of multiple emulsions can be formed by increasing the number of co-flow junctions. We are able to vary the number and size, respectively, of the inner droplets of the double emulsions by controlling fluid flow. In addition, both the diameter and the number of the individual drops at every level can be precisely controlled; this is shown by the series of triple emulsions that have up to seven innermost drops, and up to three middle drops in a single outer drop in Fig. 11b.³⁰

To demonstrate controlled release from monodisperse pNIPAM water-in-oil-in-water-in-oil (W/O/W/O) triple emulsions, we

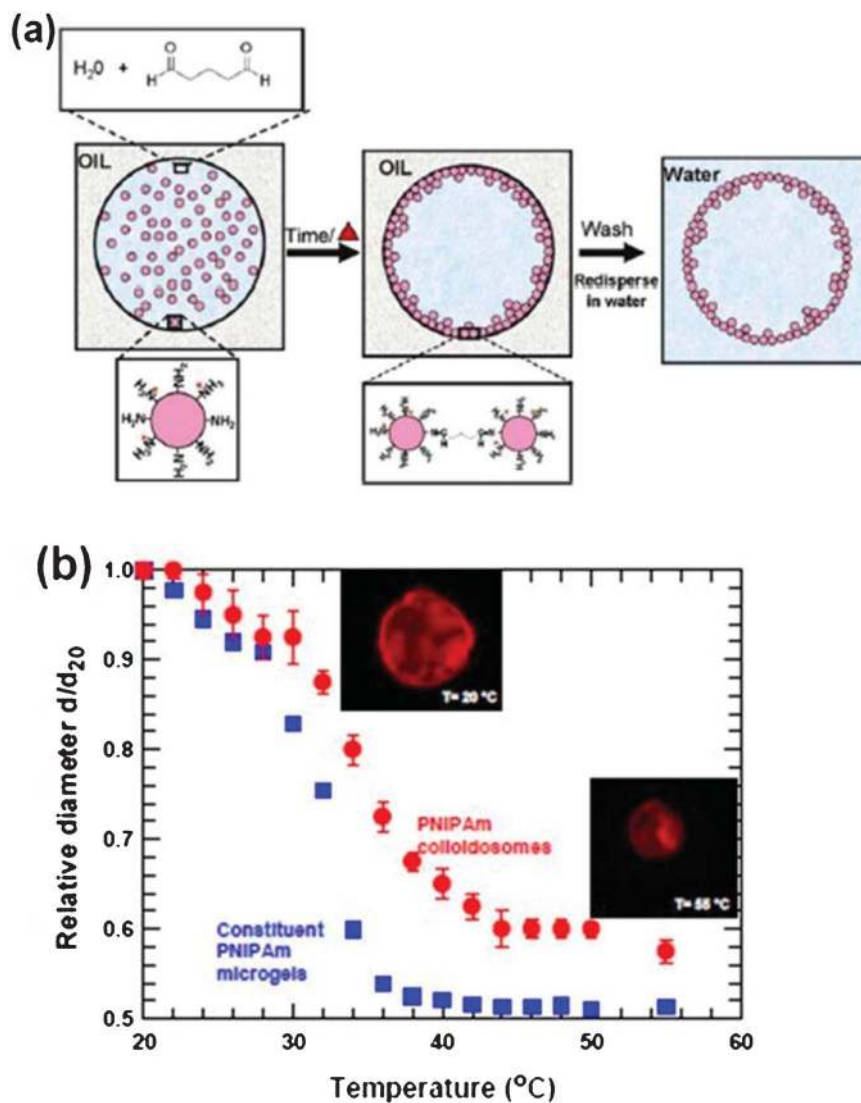


Fig. 10 (a) Schematic representation of a technique used for fabricating colloidosomes using poly(*N*-isopropylacrylamide) microgel particles as building blocks and emulsion droplets as templates. (b) Equilibrium size change of pNIPAm colloidosomes and the constituent pNIPAm microgels. Colloidosomes were dispersed in water and heated from 20 to 50 $^{\circ}C$ in fixed increments of 2 $^{\circ}C$ and then to 55 $^{\circ}C$. Images were captured after allowing the sample to equilibrate for 30 min at each temperature. The sample was then cooled down to 20 $^{\circ}C$ using the same temperature steps. Size-change data of the constituent pNIPAm microgels over the same temperature range were collected using dynamic light scattering. Adapted and reprinted with permission from ref. 29. Copyright 2010 American Chemical Society.

generate pNIPAm shells that encapsulate one oil drop that contains several water drops. Upon an increase of the temperature from 25 $^{\circ}C$ to 50 $^{\circ}C$, pNIPAm rapidly shrinks by expelling water; however, because of the incompressibility of the inner oil, the hydrogel shell breaks to provide spontaneous pulsed-release of the innermost water droplets into the continuous oil phase as shown in the series of images in Fig. 12. This structure has a Trojan-horse-like behaviour because it protects the innermost water droplets in the hydrogel shell until their temperature-induced release. This demonstrates the utility of our technique to generate highly controlled capsules with multiple internal volumes that remain separate from each other; it also highlights the potential of this microfluidic device to create highly engineered structures for controlled release of active substances.

The ability to precisely control the formation of multiple emulsions offers new opportunities to engineer novel materials.

To realize this, we create monodisperse hydrogel particles, and then we wrap these particles in aqueous polymer shells using a PDMS device. The device consists of two cross-junctions in series, as sketched in Fig. 13a.³¹ In the first junction we add a semidilute, aqueous solution of crosslinkable pNIPAm chains as the shell phase. In the second junction we add oil to form bi-layered pre-microgel drops and then set these structures by crosslinking the pNIPAm chains in the shell. The resultant particles consist of a hydrophilic polymer core that is nested in a hydrophilic polymer shell; these are both crosslinked and swollen in water but also formed from different macromolecular precursors.

To demonstrate the utility of this technique, we use a shell phase that is tagged with a green fluorescent tracer polymer, along with red-tagged core microgel particles; this allows us to visualize the formation of core-shell structures which exhibit a

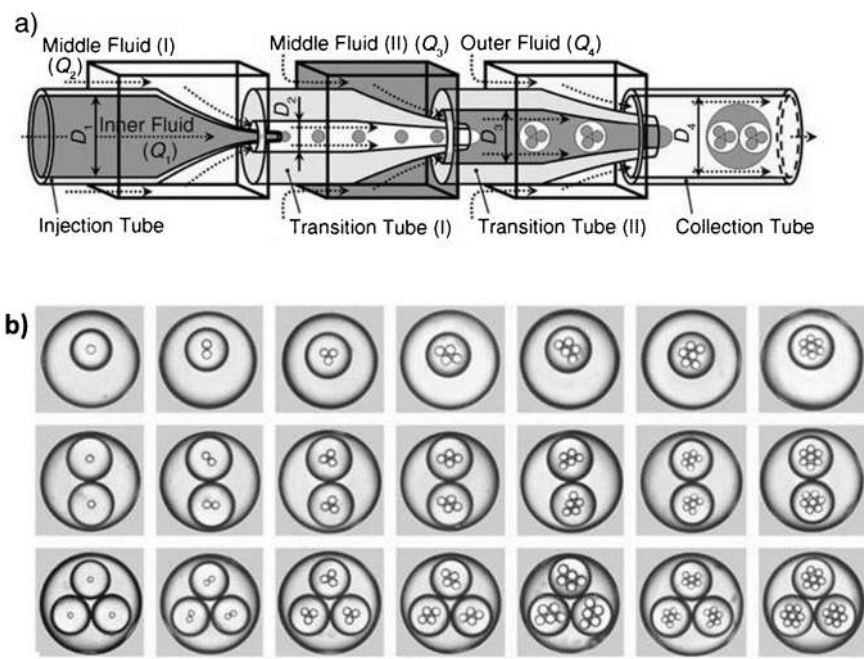


Fig. 11 Generation of highly controlled monodisperse triple emulsions. (a) Schematic diagram of the extended capillary microfluidic device for generating triple emulsions. (b) Optical micrographs of triple emulsions that contain a controlled number of inner and middle droplets. The scale bar in all images is 200 μm . Adapted and reprinted with permission from ref. 30. Copyright 2007 WILEY-VCH Verlag GmbH & Co. KGaA, Weinheim.

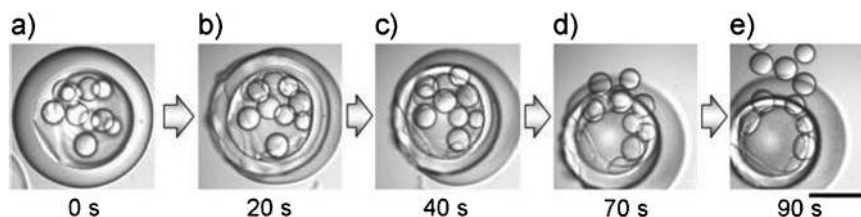


Fig. 12 Optical micrograph of a microcapsule with a shell comprised of a thermosensitive hydrogel containing aqueous droplets dispersed in oil. Upon increase of the temperature, the hydrogel shell shrinks by expelling water. This capsule was generated from a triple emulsion, where the continuous liquid is oil, the hydrogel shell is aqueous, the inner middle fluid is also oil, and the innermost droplets are aqueous. (b)–(e) Optical micrograph time series showing the forced expulsion of the oil and water droplets contained within the micro-capsule when the temperature is rapidly increased from 25 to 50 $^{\circ}\text{C}$. The time series begins once the temperature reaches 50 $^{\circ}\text{C}$. The extra layer surrounding the microcapsule in (b)–(e) is water that is squeezed out from the hydrogel shell as it shrinks. The coalescence of the expelled inner oil with the outer oil cannot be resolved, since both liquids have the same index of refraction. The scale bar is 200 μm . Reprinted with permission from ref. 30. Copyright, 2007 WILEY-VCH Verlag GmbH & Co. KGaA, Weinheim.

well-controlled number of core particles in each shell and a well-controlled shell-thickness, as shown in Fig. 13b and Fig. 13c. There is also no interpenetration of the shell material into the core, as evidenced by the middle and lower row of micrographs in Fig. 13c, which show separate visualizations of the green-labeled shells and the red-labeled cores of the microgels in the upper row. To substantiate this finding, spatially resolved profiles of the fluorescence intensity across the micrographs are visualized and plotted in Fig. 13d. These profiles show that the red-tagged core material and the green-tagged shell material are well separated.

We incorporate non-thermo-responsive polyacrylamide (pAAm) particles (not labeled) into thermo-responsive pNIPAm shells (green fluorescently labeled) to demonstrate controlled release.³¹ The shell collapses due to the volume phase transition of pNIPAm, and the core remains unaffected in response to an increase of the temperature to 35 $^{\circ}\text{C}$ which is

visualized in Fig. 14a and detailed in Fig. 14b. Due to this selective sensitivity, these particles are applicable for encapsulation and controlled release: when the pNIPAm shell is swollen, it is porous and permeable, whereas it becomes non-porous and impermeable when it collapses. By contrast, the pAAm core remains unaffected by temperature, providing stability of shape. Thus, when the shells are swollen, the particles can be loaded with hydrophilic low molecular weight or mesoscopic additives. Upon increase of the temperature, the thermo-responsive shell collapses and encapsulates these actives in the pAAm core. Then, all surrounding feed material can be removed and the loaded particles can be stored at elevated temperatures. As soon as the temperature is decreased, the actives are rapidly released. This application is substantiated in Fig. 14c, which shows a sequence of images from an experiment where RITC-tagged dextran (MW = 10 000 g mol^{-1}) is released from pAAm–pNIPAm microgels.

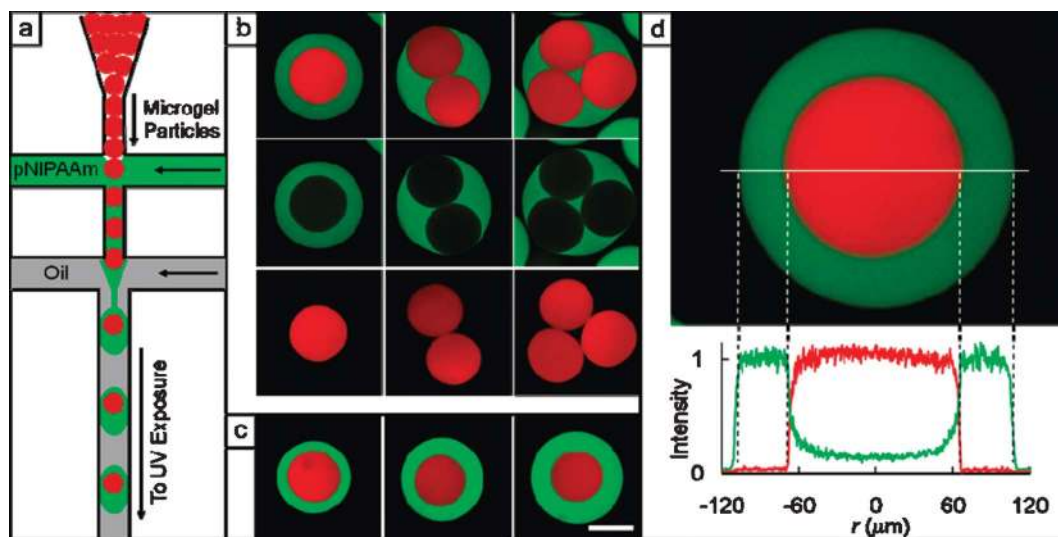


Fig. 13 Microfluidic fabrication of microgel capsules that consist of two miscible yet distinct layers. (a) Schematic of a microfluidic device forming aqueous poly(*N*-isopropylacrylamide) (pNIPAM) droplets that are loaded with a well-defined number of prefabricated particles of a similar material, pNIPAM or polyacrylamide. Subsequent gelation of the pNIPAM phase leads to microgels with a distinct core-shell architecture. (b, c) Adjusting the flow rates of the inner particle phase (red-tagged pNIPAM), the middle polymer phase (green-tagged pNIPAM), and the outer oil phase controls the number of core particles in each shell (b) as well as the shell thickness (c). Pictures in the upper row of panel b show an overlay of the micrographs in the middle and lower row, which depict separate visualizations of the green-tagged pNIPAM shell and the red-tagged pNIPAM core. (d) Spatially resolved intensity profiles of the red and green fluorescence in the single-core particle shown in panel b, evidencing only very little interpenetration of its two phases. The scale bar is 100 μm and applies to all micrographs in panels b and c. Reprinted with permission from ref. 31. Copyright 2010, American Chemical Society.

We have produced highly monodisperse and controllable pNIPAM microgels in microfluidics. Microfluidics enables a high degree of structural control to produce microgels with one or more layers. In addition, the incorporation of various

materials also enables control of microgel structure. Moreover, the ability to generate pNIPAM from precursors also increases the potential of these structures for controlled release applications.

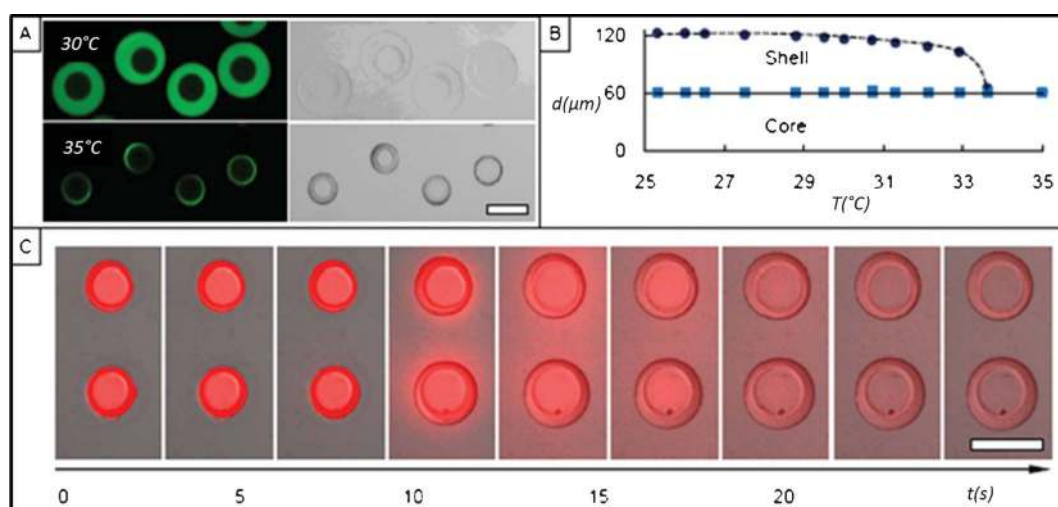


Fig. 14 Thermoresponsive behaviour of pAAm-pNIPAm core-shell microgels. (a) Fluorescence images (left column) and bright field micrographs (right column) of microgels consisting of a 60 μm nontagged pAAm core encapsulated in a green-tagged pNIPAM shell. At ambient temperatures (upper row), the shell is swollen, whereas it collapses at elevated temperatures (lower row). By contrast, the core dimension remains unaffected by the same changes of temperature. (b) Detailed plot of the particle diameter, d , as a function of temperature, T . Dark blue circles represent the diameter of the entire particle, *i.e.*, pAAm core plus pNIPAM shell, whereas light blue squares represent the sole pAAm core. The dotted lines are guides to the eye. The scale bar is 100 μm . (c) Controlled release applications of pAAm-pNIPAm core-shell microgels. Release of RITC-dextran (MW 10 000 g mol^{-1}) loaded into particles shown in (a). In the course of the first 10 s, the temperature remains above 33 $^{\circ}\text{C}$, and the particles remain sealed (left three pictures). As the temperature decreases further, a spontaneous release of the active incorporated in the particles is triggered by the reswelling of the pNIPAM shells. Reprinted with permission from ref. 31. Copyright 2010, American Chemical Society.

E Conclusions

Microfluidics production enables synthesis of a range of microparticles with distinct composition and structure, including spheres, nested multiple emulsions, and core-shell capsules; we review a variety of polymersomes and pNIPAm microparticles with these structures. Both structural and chemical modifications enable the tuning of release rates of actives from these microparticles. The principal advantage of microfluidic synthesis is the ability to independently choose the chemical composition and structure of the particles formed. While the structure of the particles is determined by the flow properties in the devices, chemical composition is determined by selecting which fluids to introduce into the device. The inclusion of biocompatible materials in these highly controlled microparticles creates opportunities to produce a variety of microparticles that are useful for advanced drug delivery.

References

- 1 R. Langer, *Nature*, 1998, **392**, 5–10.
- 2 N. K. Varde and D. W. Pack, *Expert Opin. Biol. Ther.*, 2004, **4**, 35–51.
- 3 T. M. Allen and P. R. Cullis, *Science*, 2004, **303**, 1818–1822.
- 4 C. Berkland, K. Kim and D. W. Pack, *J. Controlled Release*, 2001, **73**, 59–74.
- 5 C. Berkland, M. King, A. Cox, K. Kim and D. W. Pack, *J. Controlled Release*, 2002, **82**, 137–147.
- 6 C. Berkland, E. Pollauf, D. W. Pack and K. Kim, *J. Controlled Release*, 2004, **96**, 101–111.
- 7 K. K. Kim and D. W. Pack, *Microspheres for Drug Delivery*, in *BioMEMS and Biomedical Nanotechnology Volume 1: Biological and Biomedical Nanotechnology*, ed. M. Ferrari, A. P. Lee and L. J. Lee, Springer, New York, 2006, pp. 19–50.
- 8 D. S. Kohane, *Biotechnol. Bioeng.*, 2007, **96**, 203–209.
- 9 K. Al-Tahami and J. Singh, *Recent Pat. Drug Delivery Formulation*, 2007, **1**, 65–71.
- 10 L. Wei, C. Cai, J. Lin and T. Chen, *Biomaterials*, 2009, **30**, 2606–2613.
- 11 J. A. Champion, Y. K. Katare and S. Mitragotri, *J. Controlled Release*, 2007, **121**, 3–9.
- 12 V.-T. Tran, J.-P. Benoit and M.-C. Venier-Julienne, *Int. J. Pharm.*, 2011, **407**, 1–11.
- 13 C. Cramer, P. Fischer and E. J. Windhab, *Chem. Eng. Sci.*, 2004, **59**, 3045–3058.
- 14 A. S. Utada, A. Fernandez-Nieves, H. A. Stone and D. A. Weitz, *Phys. Rev. Lett.*, 2007, **99**, 094502.
- 15 J. M. Gordillo, Z. D. Cheng, A. M. Ganan-Calvo, M. Marquez and D. A. Weitz, *Phys. Fluids*, 2004, **16**, 2828–2834.
- 16 A. S. Utada, E. Lorenceau, D. R. Link, P. D. Kaplan, H. A. Stone and D. A. Weitz, *Science*, 2005, **308**, 537–541.
- 17 M. B. Romanowsky, A. R. Abate, A. Rotem, C. Holtze and D. A. Weitz, *Lab Chip*, 2012, **12**, 802–807.
- 18 D. E. Discher and A. Eisenberg, *Science*, 2002, **297**, 967–973.
- 19 S. H. Kim, H. C. Shum, J. W. Kim, J. C. Cho and D. A. Weitz, *J. Am. Chem. Soc.*, 2011, **133**, 15165–15171.
- 20 H. C. Shum, J. W. Kim and D. A. Weitz, *J. Am. Chem. Soc.*, 2008, **130**, 9543–9549.
- 21 H. C. Shum, Y. J. Zhao, S. H. Kim and D. A. Weitz, *Angew. Chem., Int. Ed.*, 2011, **50**, 1648–1651.
- 22 J. Thiele, A. R. Abate, H. C. Shum, S. Bachtler, S. Forster and D. A. Weitz, *Small*, 2010, **6**, 1723–1727.
- 23 R. K. Shah, J. W. Kim, J. J. Agresti, D. A. Weitz and L. Y. Chu, *Soft Matter*, 2008, **4**, 2303–2309.
- 24 S. V. Vinogradov, *Curr. Pharm. Des.*, 2006, **12**, 4703–4712.
- 25 L. Y. Chu, J. W. Kim, R. K. Shah and D. A. Weitz, *Adv. Funct. Mater.*, 2007, **17**, 3499–3504.
- 26 S. Seiffert, W. Oppermann and K. Saalwaechter, *Polymer*, 2007, **48**, 5599–5611.
- 27 X. Yu, C. Corten, H. Goerner, T. Wolff and D. Kuckling, *J. Photochem. Photobiol., A*, 2008, **198**, 34–44.
- 28 S. Seiffert and D. A. Weitz, *Soft Matter*, 2010, **6**, 3184–3190.
- 29 R. K. Shah, J. W. Kim and D. A. Weitz, *Langmuir*, 2010, **26**, 1561–1565.
- 30 L. Y. Chu, A. S. Utada, R. K. Shah, J. W. Kim and D. A. Weitz, *Angew. Chem., Int. Ed.*, 2007, **46**, 8970–8974.
- 31 S. Seiffert, J. Thiele, A. R. Abate and D. A. Weitz, *J. Am. Chem. Soc.*, 2010, **132**, 6606–6609.